JOINT INSTITUTE FOR NUCLEAR RESEARCH
Veksler and Baldin laboratory of High Energy Physics

FINAL REPORT ON THE START PROGRAMME

Unsupervised Machine Learning Approach for Particle Identification in the MPD Experiment

Supervisor: Artem Korobitsin

Student: Semenova Anastasiia
Russia, Saint-Petersburg University

Participation period: July 07 – August 23
Summer Session 2025

Dubna, 2025

Abstract

Machine learning methods are rapidly advancing and increasingly applied in experimental physics, where they provide powerful tools for analyzing complex data. One of the central challenges in high-energy nuclear physics is particle identification (PID), crucial for studying the properties of strongly interacting matter and the QCD phase diagram. In particular, separation of charged-hadrons plays a key role in reconstructing collision dynamics and understanding matter at extreme conditions.

Conventional identification techniques in MPD rely on comparing particle parameters measured by detector with theoretical curves. However, at large momenta, detector responses overlap, making the standard nσ method less reliable.

In this work, we apply an unsupervised clustering approach based on hierarchical density models to PID in the Multi-Purpose Detector at NICA. This method was chosen because it does not require labeled data, adapts to non-uniform distributions, and remains robust in overlapping areas where classical parametric approaches fail. We compare its performance with the traditional nσ method and with a supervised XGBoost classifier.

Table of Content

1. Introduction

The exploration of strongly interacting matter at extreme temperatures and densities remains one of the fundamental challenges of modern nuclear physics [1]. Particular attention is paid to the region of the QCD phase diagram at high baryon chemical potential, where novel states of matter may emerge — from the hadronic–matter to quark–gluon–plasma transition to a hypothetical critical point.

To study these phenomena, the *Nuclotron-based Ion Collider fAcility (NICA)* is being constructed at the *Joint Institute for Nuclear Research,* Dubna. NICA is designed for heavy-ion collisions at center-of-mass energies $\sqrt{s}_{NN} = 4 - 11\ GeV$. To register the interaction products *Multi-Purpose Detector (MPD)* has been engineered [2]. It designed to collect data for track reconstruction, calorimetry and charged-particle identification.

A key challenge in heavy-ion physics is *Particle Identification (PID)* — the robust separation of protons, kaons, and pions, which carry essential information about collision dynamics and matter formation mechanisms. Traditional PID methods in MPD rely on measures from the *Time Projection Chamber (TPC)* and the *Time-of-Flight detector (TOF)*. These parametric approaches compare experimental detector responses with theoretical expectations to assign particle types probabilistically.

However, conventional methods face significant limitations. At higher momenta, where theoretical curves converge, the standard nσ method becomes increasingly unreliable due to its dependence on fixed thresholds and Gaussian distribution assumptions.

Modern machine-learning methods open new opportunities by uncovering latent structure in the data and adapting to complex experimental conditions. A promising tool is the *Hierarchical Density-Based Spatial Clustering of Applications with Noise* (*HDBSCAN)* algorithm, a clustering method that requires no prior specification of the number of clusters and is resilient to non-uniform data density [3]. Its application can improve PID accuracy and complement traditional approaches without imposing parametric assumptions on distribution shapes. We suggest this method helps identify dependencies in complex areas of overlap on graphs of the distribution of key particle characteristics.

This work applies HDBSCAN to charged-hadron (p, $\overline{p}$, K^+, K^-, π^+, π^-) identification in MPD, discusses feature engineering and algorithm hyperparameters, and compares the results with existing methods.

1.1 The MPD Experiment

The Multi-Purpose Detector addresses specific challenges inherent to intermediate-energy heavy-ion collisions. Unlike ultrarelativistic regimes at higher energies, NICA collisions produce events with moderate particle multiplicities but significantly enhanced baryon-to-meson ratios. This baryon-rich environment creates unique identification challenges, as particles must be distinguished across a broad momentum range from 0.1 to 3 GeV/c where traditional separation methods often overlap. The modular design of the MPD is shown in Figure 1.

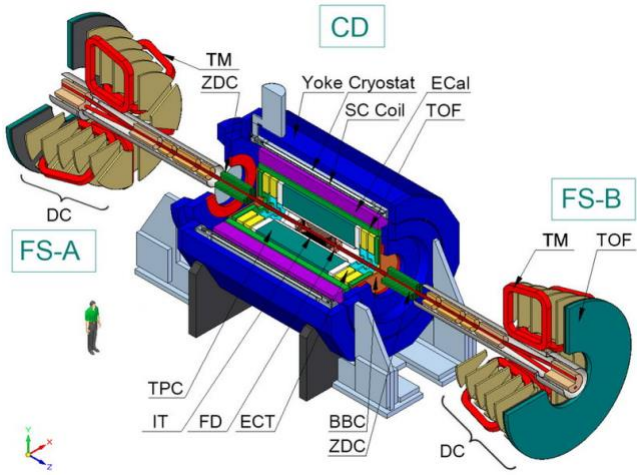

Fig. 1. MPD detector scheme

The detector's operational parameters are optimized for studying the baryon-rich region of the QCD phase diagram, where first-order phase transitions and critical phenomena may manifest through specific particle production patterns and correlation signatures that demand robust identification capabilities.

The joint use of TPC and TOF enables precise reconstruction of the kinematics of collision products.

1.2.1 Time Projection Chamber

The Time Projection Chamber is the primary tracking detector of MPD and simultaneously serves as a spectrometer for energy loss. Its main function is the high-precision reconstruction of trajectories of charged particles traversing a gas volume. TPC operation relies on two fundamental effects: *gas ionization* by the passing particle and *electron drift* in an electric field.

As a charged particle passes through the gas, it excites and ionizes the medium, creating electrons and ions along its path. An electric field applied along the detector axis drives the electrons toward a segmented anode plane, where the signals are recorded with high spatial and temporal resolution. Combining drift time with position measurements enables reconstruction of the three-dimensional trajectory.

In addition, the TPC measures the energy loss (dE/dx), which depends on the particle's speed and mass according to the *Bethe–Bloch law:*

$$-\frac{dE}{dx} = Kz^2\frac{Z}{A}\frac{1}{\beta}\left(\frac{1}{2}\ln\frac{2m_e c^2\beta^2\gamma^2 T_{max}}{I^2} - \beta^2 - \frac{\delta}{2}\right),$$

where $K = 4\pi N_A r_e^2 m_e c^2, z -$ particle charge, $\beta = v/c,\ \gamma -$ Lorentz factor, $T_{max} -$ the maximum transferable energy to an electron, $I -$ the mean ionization potential, $\delta -$ the density-effect correction.

Example of data collecting from TPC is shown in Figure 2. These measurements provide a direct method to distinguish particles of different masses at the same momentum — a foundation of classical PID. The precision of *dE/dx* depends on the number of samples along the track, gas properties, and the stability of the electric field.

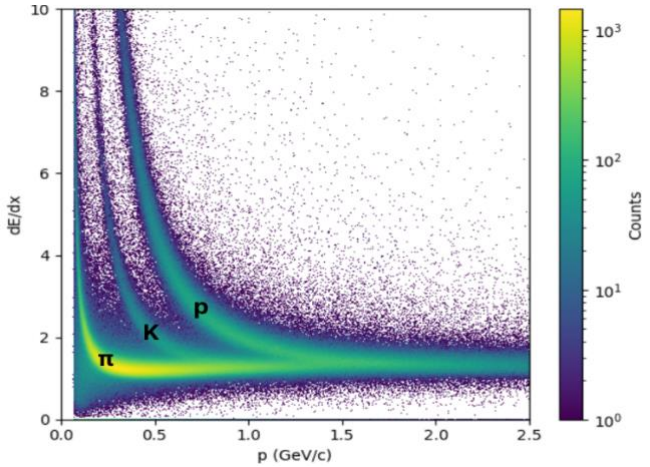

Fig. 2. Distribution of ionization losses vs. total momentum for p, K, π

In MPD, the TPC covers a wide angular range and provides sub-millimeter spatial resolution. It is particularly effective at low and intermediate momenta, where the dE/dx separation between protons, kaons, and pions is most pronounced. Thus, the TPC combines tracking and spectrometric functions and provides a robust basis for integration with other PID subsystems.

1.2.2 Time of Flight detector

The Time-of-Flight system complements the TPC by extending PID capabilities into the intermediate and high momentum regions where dE/dx alone becomes less discriminating. By calculating the total moment from the TPC and measuring the time t it takes a particle to traverse a known path length L from the interaction point to the TOF detector in order to calculate the kinematic characteristics of the particle:

$$\beta = \frac{L}{ct}, \qquad m^2 = p^2\left(\frac{1}{\beta^2} - 1\right).$$

The MPD TOF employs fast sensors with timing resolution of order tens of picoseconds, enabling precise mass determination and separation of protons, kaons, and pions where TPC-based separation degrades. The data obtained from TOF can be viewed in Figure 3.

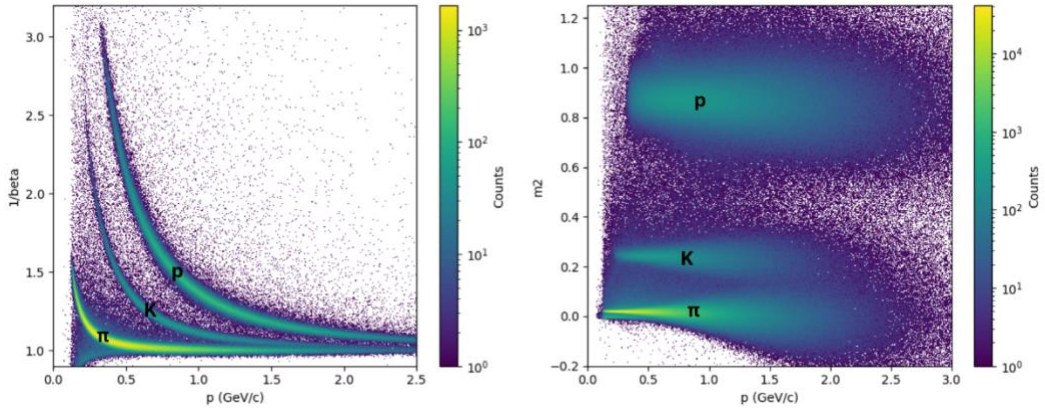

Fig. 3 Distribution of $1/\beta$ (left) and m^2 (right) versus total momentum for p, K, π

TOF plays a crucial role in *combined PID*: time-of-flight information is used together with TPC dE/dx to form a multidimensional feature space, which significantly reduces overlap between particle types and improves identification reliability.

The main TOF uncertainties are associated with determining the interaction start time t_0 and variations of track length in the magnetic field. These factors define the achievable timing resolution and thus the separation power.

Nevertheless, TOF effectively complements the TPC, broadening the PID reach and reducing species mixing in critical momentum intervals.

2. Particle Identification in MPD

After reconstructing the trajectories and kinematic properties of charged particles in MPD using TPC and TOF, one obtains a primary experimental dataset. However, knowledge of track coordinates, flight times, and energy losses by itself does not directly reveal the particle type. Detection records a signal; identification interprets it in terms of species. In high-multiplicity events, with substantial overlap of proton, kaon, and pion distributions, automated PID becomes nontrivial.

2.1 Physical principles of PID

PID in tracking and timing systems is based in the relations between a particle's velocity, mass, and charge. The movement of a charged hadron in the TPC magnetic field allows its momentum p to be determined, while dE/dx in the gas follows the Bethe–Bloch law and depends mainly on $\beta = v/c$. Combined with the flight time t from TOF, one obtains the velocity and, together with p, reconstructs the square mass of the particle.

The difference between β and ionization losses of protons, kaons, and pions at the same momentum enable their separation within certain boundaries.

2.2 Current MPD PID methods

In practice, MPD PID employs the $n\sigma$ *method* [3]. For each particle hypothesis, a theoretical dependence (e.g., dE/dx vs. p or $1/\beta$ vs. p) is constructed, and experimental points are compared to these curves.

Deviations are normalized to the experimental resolution σ, calculating a dimensionless variable n. For pions, for example according to data on ionization losses:

$$n_\pi = \frac{(dE/dx)_{meas} - (dE/dx)_\pi(p)}{\sigma_\pi(p)},$$

same for kaons and protons. A similar formula is used for other kinematic characteristics of a particle $(1/\beta, m^2)$. If $|n|$ for a given hypothesis falls within a specified range (e.g., $|n| < 3$), the particle is classified accordingly. This method is simple and transparent, and it separates species where their curves diverge appreciably.

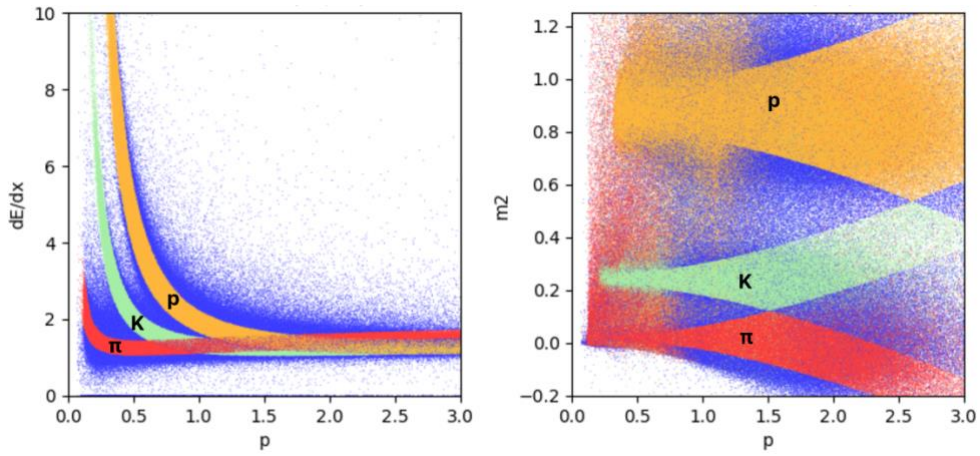

Fig. 4. Particle identification using the nσ method

However, at higher momenta ($p > 1.5\ Gev/c$), differences in dE/dx and m^2 diminish, intervals overlap (Fig. 4), and misidentification rates increase.

The Bayesian approach for PID also exists, where detector responses are combined probabilistically, but it is not considered in this study due to the impossibility of making direct comparisons: the implementation is not currently available for external analysis.

These limitations motivate the search for more universal analysis methods, including machine-learning algorithms.

3. Machine Learning Approach for PID

Classical PID in MPD, based on TPC dE/dx and TOF timing, suffers at high multiplicities due to statistical fluctuations and natural signal spread. Reliance on a priori distribution shapes and fixed decision boundaries limits performance.

Machine learning — in particular, clustering — avoids rigid parameterizations by using the data's intrinsic structure to identify groups corresponding to different species. Physically, particles of one species form clusters in a multidimensional feature space (e.g., p, $1/\beta$, m^2) with statistical dispersion defined by the detector resolution. Visual inspection reveals well-separated clusters, motivating algorithms that can discover complex structures without knowing the number of classes in advance.

Because particle clusters often lie on *curved manifolds* with heterogeneous densities and different local spreads, the *HDBSCAN* algorithm is particularly attractive. By relying on mutual-reachability distances and a hierarchy built from a minimum-spanning tree, HDBSCAN normalizes local density variations and can distinguish particle species even in challenging PID regions.

Advantages of HDBSCAN for PID include:

- a non-parametric, density-based model compatible with the curved geometry of species manifolds;
- natural handling of detector noise and artifacts;

- adaptation to non-uniform densities, robustly treating both dense and sparse cluster regions;
- scalability suitable for streaming data processing.

Thus, HDBSCAN is a promising tool for MPD PID tasks.

3.1 HDBSCAN

HDBSCAN extends DBSCAN with a hierarchical density model. The key idea is that clusters are regions where the data density significantly exceeds that of the surrounding noise. By moving from a fixed density scale to a hierarchy, HDBSCAN identifies clusters of varying shapes and densities and yields a stable partition [4, 5].

HDBSCAN algorithm:

1. Core-distance. For each data point $x_i \in X$, compute the distance to its k-th nearest neighbor (where min_samples $=$ k):

$$core_k(x_i) = \min\{r || \{x_j : d(x_i, x_j) \le r\}| \ge k\},$$

where $d(x_i, x_j) = \sqrt{\sum_{k=1}^{d} \left(x_i^{(k)} - x_j^{(k)}\right)^2}$, $x_i, x_j \in \mathrm{R}^{\mathrm{d}}$ – the euclidean metric.

The core-distance characterizes the local density around the point: small $core_k(x_i)$ means high density, large $core_k(x_i)$ indicates sparse regions.

2. Mutual reachability distance. For each pair of points x_i, x_j, define the mutual reachability distance – modified metric used for graph construction:

$$d_{mreach,k}(x_i, x_j) = \max\{core_k(x_i), core_k(x_j), d(x_i, x_j)\},$$

This metric balances density variations:

- if either point lies in a low-density region, the distance is inflated;
- if both points lie in dense regions, the value reduces to the original metric $d(x_i, x_j)$.

3. Construction of the weighted graph. Consider the complete weighted graph $G = (V, E)$, where vertices V correspond to the data points $\{x_1, \dots, x_N\}$, and the weight of each edge $(x_i, x_j) \in E(x_i, x_j)$ is equal to the mutual reachability distance:

$$w(x_i, x_j) = d_{mreach,k}(x_i, x_j).$$

4. Minimum Spanning Tree (MST). Compute the minimum spanning tree T of the graph G:

$$T = \arg\min_{T \subseteq G} \sum_{(x_i, x_j) \in T} w(x_i, x_j).$$

The MST preserves the connectivity of the dataset while minimizing the total mutual reachability distance.

5. Hierarchical clustering (condensed tree). Sort the edges of the MST by increasing weight and remove them one by one. Each removal (x_i, x_j) with weight w causes the tree to split, producing new clusters.

Introduce the density parameter:

$$\lambda = \frac{1}{d_{mreach,k}(x_i, x_j)}.$$

At high λ (low distances) clusters are small and dense; as λ decreases, clusters merge. This process yields a hierarchical dendrogram of density-based clusters.

6. Cluster stability. For a cluster C that exists over the interval $[\lambda_{\min}(C), \lambda_{\max}(C)]$, its stability is defined as the sum of the lifetimes of its member points:

$$\text{Stability}(C) = \sum_{x_i \in C} \left(\lambda_{\max}(x_i) - \lambda_{\min}(C)\right),$$

Where $\lambda_{\max}(x_i)$ is the largest value of λ for which point x_i belongs to cluster C, and $\lambda_{\min}(C)$ is the value of λ at which C is formed.

A cluster is considered more meaningful if it persists across a wide range of density thresholds.

7. Extraction of the optimal clustering. Once the condensed cluster tree has been constructed, HDBSCAN selects clusters by maximizing their *stability*:

$$\mathcal{C}^* = \arg\max_{\mathcal{C}} \sum_{C \in \mathcal{C}} \text{Stability}(C),$$

where $\mathcal{C}$ is a family of admissible, non-overlapping clusters.

However, in practice the algorithm introduces an additional parameter — cluster_selection_epsilon — which controls the smoothness of cluster boundaries.

Formally, instead of discarding points immediately when their $\lambda(x_i)$ falls below $\lambda_{\min}(C)$, we allow them to remain in the cluster provided that

$$\lambda(x_i) \geq \lambda_{\min}(C) - \varepsilon_\lambda, \qquad \varepsilon_\lambda = \frac{1}{\text{cluster\_selection\_epsilon}}$$

This relaxation allows clusters to absorb slightly less dense "tails" of points, which is particularly useful when the data distribution is smeared due to detector resolution or measurement errors.

All points that do not belong to any stable cluster are labeled as noise (typically assigned label -1).

3.1.1 Feature selection

HDBSCAN depends critically on the *geometry* of the data: it operates on local densities and topology. Features choice is therefore crucial.

We use physically motivated features:

$$X = \{p, 1/\beta, m^2, q\},$$

where $p -$ particle total momentum, $1/\beta -$ is the inverse velocity, m^2 is the squared mass, $q -$ charge of the particle.

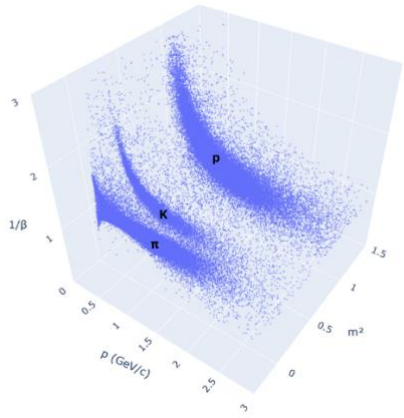

Fig. 5. Distribution of particles in the feature space taken for HDBSCAN training

This combination creates a space in which protons, kaons, and pions occupy in distinct, well-separated regions forming clusters (Fig. 5). Alternative feature choices degraded performance: geometry became less pronounced and clusters merged. The selected set is thus near-optimal, aligning with Bethe–Bloch expectations.

3.1.2 Data preprocessing

The features span different numeric ranges:

$$p \in [0; 3]\ (Gev/c\ ), \qquad m^2 \in [0; 1.25]\ (Gev^2/c^4), \qquad 1/\beta \in [1; 3.2].$$

Because HDBSCAN is distance-sensitive, we rescale features to preserve their relative importance and ensure proper algorithm behavior:

$$p_{scaled} = 50 \cdot p, \qquad m^2_{scaled} = 1250 \cdot m^2, \qquad (1/\beta)_{scaled} = 500 \cdot (1/\beta).$$

The coefficients make the dynamic ranges comparable, while deliberately assigning a smaller scaling "weight" to momentum so that sparse regions at higher p retain their density structure and cluster membership. This preserves data topology and sharpens cluster boundaries.

3.1.3 Hyperparameters selection

The key HDBSCAN hyperparameters are:

- $min\_cluster\_size$: the minimum number of points required to form a stable high-density region. Too small → noise fluctuations; too large → true clusters are merged or lost.
- $cluster\_selection\_epsilon$: controls the merging of closely related structures and the granularity of the final partition.

Optimization study for these parameters was conducted using the *Optuna framework* [6] to efficiently navigate the hyperparameter space via stochastic sampling. Optuna efficiently navigates the complex parameter space by employing a technique known as Bayesian optimization. It builds a probabilistic model of the objective function and uses it to direct the search towards the most promising hyperparameters. A key feature of Optuna is «pruning», which allows it to automatically terminate underperforming trials before they complete, leading to a substantial increase in optimization efficiency.

An initial wide scan (min_cluster_size $\in [0,200]$, cluster_selection_epsilon $\in [0,200]$) identified unstable regimes (collapse to a single cluster or over-fragmentation) and promising regions. Then search for the specified area (min_cluster_size $\in [40;70]$, cluster_selection_epsilon $\in [35;55]$ gave the optimal values:

$$min\_cluster\_size = 49, \qquad cluster\_selection\_epsilon = 45.49.$$

The optimization criterion was the macro-averaged true-positive fraction:

$$TP = \sum_{type=\pi,K,p} \frac{TP_{type}}{all_{type}},$$

where $TP_{type} -$ is the number of correctly identified particles of a given type and all_{type} is the total number of particles of that type..

3.2 Training and clustering results

The simulated data used to train HDBSCAN were obtained by the Monte Carlo method using the generators UrQMD and underwent the entire chain of reconstructions, on the condition of real Bi-Bi collisions of the MPD experiment with √sNN=9.2 GeV. Dataset contained $p, \overline{p}, K^+, K^-, \pi^+, \pi^-$. For each particle, four features were used: total momentum p, inverse velocity $1/\beta$, squared mass m^2 and charge. After rescaling to balance their contributions to the distance metric, the data were given to a HDBSCAN with $min\_cluster\_size = 49$ and $cluster\_selection\_epsilon = 45.49$, as obtained by Optuna.

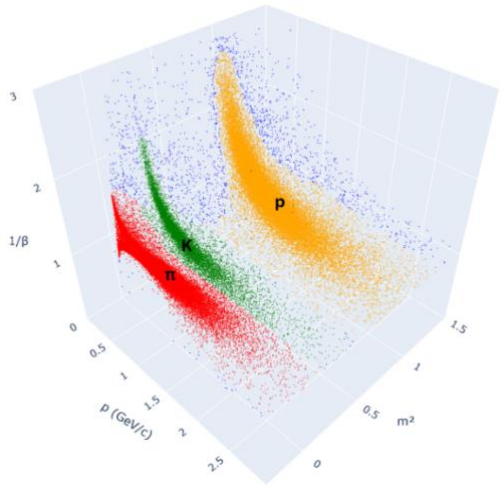

Fig. 6. Distribution of particles between clusters (red cluster – π, green cluster – K, yellow cluster – p) after HDBSCAN training in feature space $\{p, 1/\beta, m^2\}$

Clustering in the feature space produced three stable groups shown on Fig. 6 corresponding to protons, kaons and pions.

Importantly, the algorithm faithfully reconstructed the data topology, reproducing the Bethe–Bloch–driven species trends in the parameter space *without* explicitly encoding the underlying physics. HDBSCAN thus demonstrated the ability to extract physical regularities directly from experimental observables.

4. Comparison

To evaluate HDBSCAN effectiveness, we performed systematic comparison with two established approaches: the traditional nσ method currently implemented in MPD PID analysis and PID with XGBoost [7] as a representative supervised machine learning technique.

Table 1. shows summarizes the quantitative performance comparison across all particle types:

Method	Efficiency	Number of classified points	Noise	Percentage of classified points	Training Requirements
HDBSCAN	0.96	1473070	26930	98%	Unsupervised
XGBoost PID	0.99	1500000	0	1.00%	Labeled data required
MPD PID	0.89	1422035	77965	0.94%	Parameter tuning

Table. 1. Comparison of methods of PID

While XGBoost PID achieves highest overall performance, it requires extensive labeled training data and lacks physical interpretability. HDBSCAN provides competitive results without supervision, maintaining direct connection to underlying physics principles.

The confusion matrices (shown on Fig. 7) reveal important insights about misclassification patterns. All methods show elevated confusion between kaons and pions in the intermediate momentum range, where their kinematic signatures overlap significantly. HDBSCAN demonstrates exceptional pion identification efficiency across momentum ranges.

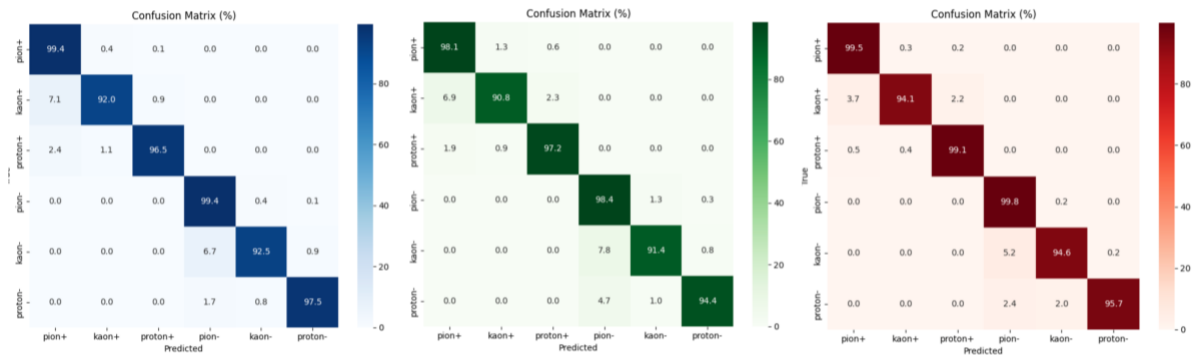

Fig. 7. Confusion matrices of HDBSCAN, MPD PID and PID with XGBoost (from left to right)

A momentum-dependent analysis provides deeper insights into method performance (Fig. 8). In the area of the average momentum range all three methods work relatively well due to the clear separation of theoretical curves and sufficient statistics. PID with XGBoost shows best effectiveness for all particle types and momentum region. While HDBSCAN

demonstrates improved performance over the nσ method, successfully handling the non-linear cluster boundaries and displaying resembling to XGBoost behavior.

However, the low and high momentum range presents the most significant challenges for particle identification.

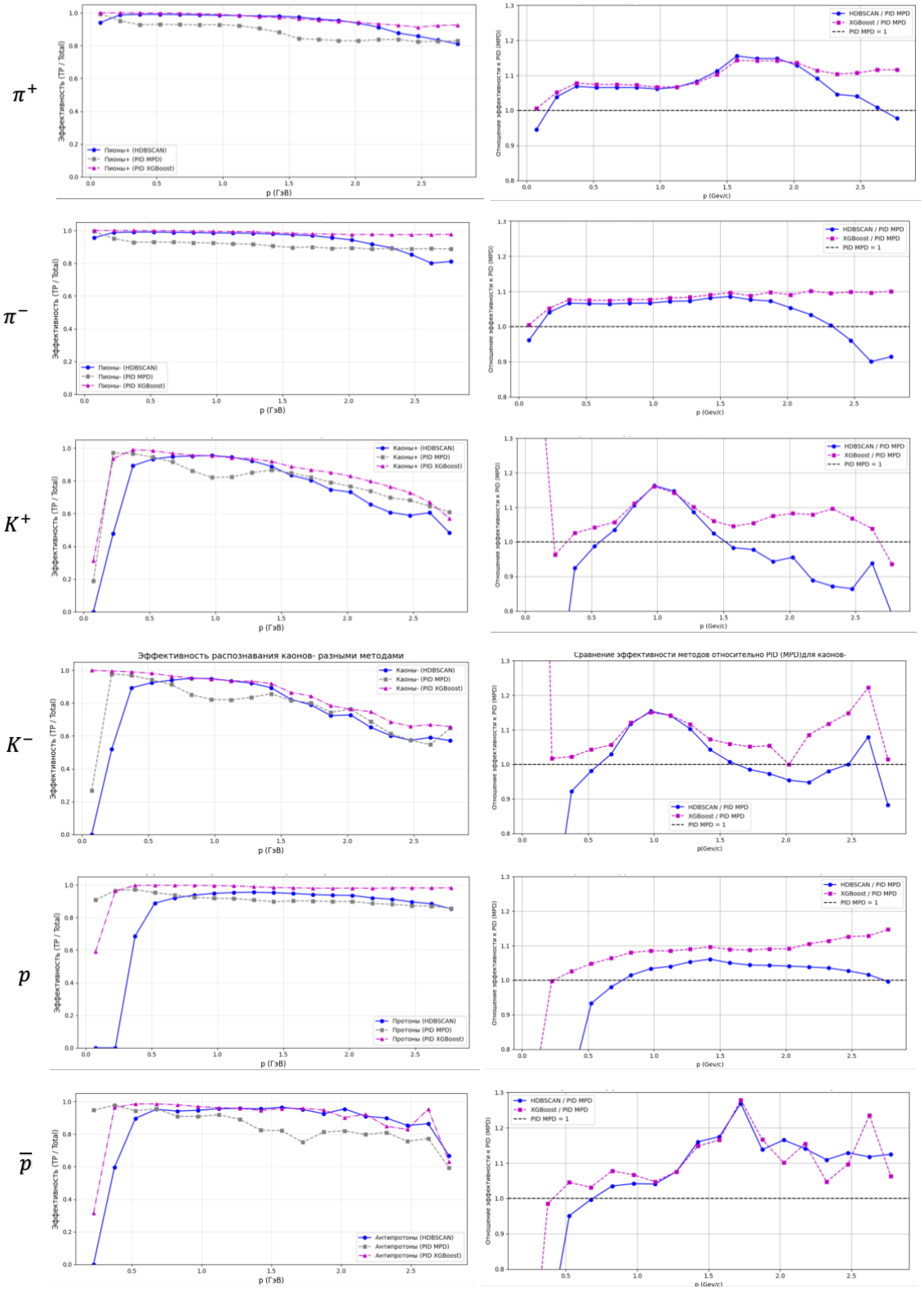

Fig. 8. Efficiency graphs (on the left) and efficiency graphs relative to the PID (on the right) from top to bottom for π+, π-, K^+, K^-, p, $\bar{p}$.

The low momentum region shows problem of current feature selection for HDBSCAN training. Lack of statistics of $1/\beta$ and m^2 for $p < 0.4$ not allowed clustering method reveal full potential and identify stable dependencies. However, it can be noted that this is not the case for particles with high statistics (π^+, π^-), and the method gives results no worse than MPD PID.

At momentum $0{,}5 < p < 2{,}0$ HDBSCAN confidently dominates $n\sigma$ method and can be comparable in efficiency with XGBoost PID.

At the high momentum region parametric methods struggle when theoretical curves converge, but the density-based clustering approach maintains effectiveness. Of course, difficulties arise for some types of particles, but this could be solved by additional manipulations.

Analysis of particle-antiparticle identification shows consistent performance of machine learning methods across charge states. The HDBSCAN algorithm maintains efficiency for both positive and negative charged particles, indicating robust charge-independent clustering that relies primarily on kinematic rather than charge-dependent signatures.

Examining the method-specific advantages, HDBSCAN's non-parametric nature eliminates dependence on rigid theoretical assumptions while maintaining physical interpretability. The algorithm adapts automatically to local data density variations and provides inherent outlier detection capabilities. In contrast, traditional methods suffer from threshold sensitivity and critical dependence on Gaussian assumptions for measurement uncertainties, particularly problematic when these assumptions are violated.

The implementation represents more than just a technical improvement. HDBSCAN's ability to identify patterns in particle physics data demonstrates the potential for discovering new relationships within existing datasets. By improving data topology through better clustering, the method enhances the quality of training data for subsequent analyses, creating a positive feedback loop for overall analysis performance.

The implementation of HDBSCAN in MPD analysis represents a paradigm shift from model-dependent to data-driven particle identification. This transition is particularly significant for rare process studies with enhanced sensitivity for low-statistics measurements, systematic uncertainty reduction through decreased dependence on theoretical parameterizations, and detector performance studies with improved understanding of detector response through data-driven approaches.

6. Conclusion

This work successfully demonstrates that modern unsupervised machine learning techniques can not only match but exceed the performance of traditional physics-based methods in particle identification tasks. The HDBSCAN implementation provides a robust, scalable, and physically meaningful approach to charged particle identification in the challenging environment of heavy-ion collisions.

The results validate the potential for broader application of density-based clustering methods in experimental physics, opening new avenues for data-driven discovery in fundamental research. As experimental datasets continue to grow in size and complexity, such adaptive algorithms will become increasingly essential for maximizing the scientific output of major physics facilities.

The study establishes HDBSCAN as a viable alternative to traditional particle identification methods, particularly valuable in regions where conventional approaches face limitations. The algorithm's ability to maintain physical interpretability while adapting to complex data structures positions it as a promising tool for future high-energy physics analyses. The success of this implementation suggests that similar density-based approaches could find applications across a broader range of experimental physics challenges, from detector calibration to event reconstruction optimization.

References

1. Kekelidze, V. "Project NICA at JINR: status and prospects." *Physics of Particles and Nuclei*, 48(5), 727-741.
2. Golosov, O. MPD Collaboration. "Multi-Purpose Detector to study heavy-ion collisions at NICA." *Nuclear Instruments and Methods in Physics Research Section A*, 1014, 165735.
3. https://git.jinr.ru/nica/mpdroot/tree/pro/mpdpid.
4. McInnes, L., Healy, J., & Astels, S. (2017). hdbscan: Hierarchical density based clustering. *Journal of Open Source Software*, 2(11), 205.
5. https://hdbscan.readthedocs.io/en/latest/how_hdbscan_works.html
6. Akiba, T., Sano, S., Yanase, T., Ohta, T., & Koyama, M. (2019). Optuna: A next-generation hyperparameter optimization framework. In *Proceedings of the 25th ACM SIGKDD international conference on knowledge discovery & data mining* (pp. 2623-2631).
7. Korobitsin, A., et al. (2024). "Machine learning approaches for particle identification in the MPD experiment at NICA." *Physics of Particles and Nuclei Letters*, 21(3), 445-458.